

Optical Mapping of Ventricular Defibrillation in Isolated Swine Right Ventricles: Demonstration of a Postshock Isoelectric Window After Near-Threshold Defibrillation Shocks

Nina C. Wang, Moon-Hyoung Lee, Toshihiko Ohara, Yuji Okuyama, Gregory A. Fishbein, Shien-Fong Lin, Hrayr S. Karagueuzian and Peng-Sheng Chen

Circulation. 2001;104:227-233

doi: 10.1161/01.CIR.104.2.227

Circulation is published by the American Heart Association, 7272 Greenville Avenue, Dallas, TX 75231

Copyright © 2001 American Heart Association, Inc. All rights reserved.

Print ISSN: 0009-7322. Online ISSN: 1524-4539

The online version of this article, along with updated information and services, is located on the World Wide Web at:

<http://circ.ahajournals.org/content/104/2/227>

Permissions: Requests for permissions to reproduce figures, tables, or portions of articles originally published in *Circulation* can be obtained via RightsLink, a service of the Copyright Clearance Center, not the Editorial Office. Once the online version of the published article for which permission is being requested is located, click Request Permissions in the middle column of the Web page under Services. Further information about this process is available in the [Permissions and Rights Question and Answer](#) document.

Reprints: Information about reprints can be found online at:
<http://www.lww.com/reprints>

Subscriptions: Information about subscribing to *Circulation* is online at:
<http://circ.ahajournals.org/subscriptions/>

Optical Mapping of Ventricular Defibrillation in Isolated Swine Right Ventricles

Demonstration of a Postshock Isoelectric Window After Near-Threshold Defibrillation Shocks

Nina C. Wang, BA; Moon-Hyoung Lee, MD; Toshihiko Ohara, MD; Yuji Okuyama, MD; Gregory A. Fishbein, BA; Shien-Fong Lin, PhD; Hrayr S. Karagueuzian, PhD; Peng-Sheng Chen, MD

Background—Investigators who studied ventricular defibrillation by use of optical mapping techniques failed to observe an initial defibrillation event (isoelectric window or quiescent period) shown by electrode mapping studies. This discrepancy has important implications for the mechanisms of defibrillation. The purpose of the present study was to demonstrate an optical equivalent of an isoelectric window after a near-threshold defibrillation shock.

Methods and Results—We studied 10 isolated, perfused swine right ventricles. Upper limit of vulnerability was determined by shocks on T waves. A 50% probability of successful defibrillation (DFT50) was determined with an up-down algorithm. Immediately after unsuccessful defibrillation shock, new wavefronts were generated. When the shock strength was low, immediate reinitiation of reentry and ventricular fibrillation might occur without a postshock isoelectric window. However, if the shock strength was within 50 V of DFT50 (near-threshold), a synchronized activation occurred, followed by organized repolarization that ended 64 ± 18 ms after shock. After a period of quiescence (18 ± 24 ms), activation recurred 83 ± 33 ms after shock and reinitiated ventricular fibrillation. Similar patterns of activation, including a quiescent period, were observed after shock was applied on the T wave of the paced beat that induced ventricular fibrillation. Upper limit of vulnerability correlated well with DFT50.

Conclusions—In isolated swine right ventricles, an optical equivalent of an isoelectric window exists after near-threshold defibrillation shocks. These findings support the idea that a near-threshold defibrillation shock terminates all activation wavefronts but fails to halt ventricular fibrillation because the same shock reinitiates ventricular fibrillation after an isoelectric window. (*Circulation*. 2001;104:227-233.)

Key Words: action potentials ■ mapping ■ electrical stimulation ■ electrophysiology ■ death, sudden

Mechanisms of ventricular defibrillation have been studied with both electrode and optical mapping techniques. Although electrode mapping studies demonstrated a postshock isoelectric window (quiescent period) after threshold or near-threshold defibrillation shocks,¹⁻³ optical mapping studies failed to show such an initial defibrillation event.⁴ Depending on presence or absence of a postshock isoelectric window, 2 different hypotheses were proposed to explain mechanisms of defibrillation.^{5,6} Presence of an isoelectric window after a failed defibrillation shock led to the proposal that a shock terminates all activation wavefronts but fails to halt ventricular fibrillation (VF) because the same shock reinitiates VF. Because electrical shock applied during a critical (vulnerable) period can induce reentry and VF,⁷ the “reinitiation” scenario was also supported by the observation that the upper limit of vulnerability (ULV) correlates well with the defibrillation threshold in both animals^{8,9} and hu-

mans.¹⁰ This correlation suggests that for a shock to defibrillate successfully, it must exceed the ULV throughout both ventricles so that reentry and VF are not reinitiated (ULV hypothesis of defibrillation). A postshock isoelectric window was consistently observed in studies with electrode mapping techniques.¹ However, optical mapping studies by Kwaku and Dillon⁴ did not show the optical equivalent of an isoelectric window after failed shock. Absence of an isoelectric window prompted them to propose the “progressive depolarization hypothesis.”⁵ According to that hypothesis, shocks can depolarize the ventricles, and this depolarization may propagate immediately to continue or instigate VF. Progressively stronger shocks achieve defibrillation by progressively prolonging and synchronizing repolarization. In the present study, we sought to resolve apparent discrepancies among different studies on the events that immediately follow a defibrillation shock in isolated perfused swine right ventri-

Received January 2, 2001; revision received March 21, 2001; accepted March 26, 2001.

From the Division of Cardiology (N.C.W., M.-H.L., T.O., Y.O., G.A.F., H.S.K., P.-S.C.), Department of Medicine, Cedars-Sinai Medical Center and University of California—Los Angeles, Los Angeles, Calif; and Department of Physics and Astronomy (S.-F.L.), Vanderbilt University, Nashville, Tenn.

Correspondence to Peng-Sheng Chen, MD, Room 5342, Cedars-Sinai Medical Center, 8700 Beverly Blvd, Los Angeles, CA 90048. E-mail chenp@csmc.edu

© 2001 American Heart Association, Inc.

Circulation is available at <http://www.circulationaha.org>

cles (RVs). Specifically, we sought to determine whether an optical equivalent of an isoelectric window exists after failed defibrillation shocks.

Methods

Tissue Preparation

Ten farm pigs (25 to 32 kg) of either sex were used in the study. Details of this model have been reported elsewhere.¹¹ Briefly, each pig was anesthetized and its heart quickly removed. Right coronary artery was cannulated and perfused with Tyrode's solution ($37\pm 0.5^\circ\text{C}$, pH 7.4 ± 0.5). RV was then excised and placed in the tissue chamber with the epicardial surface facing up. Two Guidant Endotak leads were placed at 2 ends of the tissue chamber. Defibrillation shocks were delivered with a Ventritex HVS-02 external defibrillator, which delivers biphasic truncated exponential waveform shocks of fixed-pulse duration (6 ms) and variable tilt. Leading-edge voltage of the second (negative) phase was one half of the residual value of the first (positive) phase. Each phase was 3 ms.

Optical Mapping

The optical mapping system used in the present study was similar to the one described previously.¹² RVs were stained for 20 minutes with 0.5 to 2 $\mu\text{mol/L}$ di-4-ANEPPS (Molecular Probes, Inc) added to the Tyrode's solution. To reduce tissue contraction, 5 mmol/L of diacetyl monoxime (DAM) was used. In experiments 1 through 3, fluoresced and scattered light was collected with a charge-coupled device camera (Dalsa, Inc) operating at ≈ 258 frames per second (3.75-ms sampling interval) and acquiring from 96×96 sites simultaneously over a $35\times 35\text{-mm}^2$ area, which resulted in spatial resolution of $0.36\times 0.36\text{ mm}^2$ per pixel. In experiments 4 through 10, the charge-coupled device camera was programmed to acquire either from 64×64 sites at 869 frames per second ($n=4$) or from 128×128 sites at 463 frames per second ($n=3$).

Study Protocol

The 50% probability of successful defibrillation (DFT50) was determined with an up-down algorithm¹³ with biphasic truncated exponential waveform shocks of fixed-pulse duration (6 ms). To determine ULV, RVs were paced at 400-ms cycle length and shocks were delivered at varying coupling intervals (from 130 to 380 ms at 20-ms increments) after the last paced beat. ULV was the lowest shock strength that failed to induce VF at any coupling interval. At the end of study, RVs were incubated for 30 to 45 minutes in phosphate-buffered (pH 7.4) triphenyl tetrazolium chloride¹⁴ (14 g/L) to determine viability.

Data Analysis

Fluorescence signals were baseline-subtracted, inverted, normalized, and spatially averaged with the signals of 8 neighboring pixels to reduce noise. Amplitude of the optical signals may vary from site to site in the same tissue because of factors such as uneven distribution of epicardial fat. To normalize the signal, we identified minimal and maximal amplitudes for each pixel and assigned them amplitudes of 0 and 255, respectively. We rescaled all signals on that pixel according to this new scale. Each pixel was assigned a shade of gray between white (representing fully depolarized state) and black (representing fully repolarized state).

For computer-assisted automatic detection of wavebreak, we defined occurrence of wavebreak in a propagating wavelet as a point at which activation wavefront and repolarization waveback join together. The computer finds every adjacent pair of pixels in the frame that crosses the average value of the data. If the intensity of the data on which the line coincides is increasing, that edge is identified as the wavefront and colored red. If it is decreasing, the edge is identified as the waveback and colored blue.¹⁵ The point at which the red line meets the blue line is a wavebreak.

Results are expressed as mean \pm SD. Student's *t* tests and Pearson correlation coefficients were calculated to compare means between

DFT50 and ULV. ANOVA with Newman-Keuls test was used for multiple comparisons. $P\leq 0.05$ was considered significant.

Definition of Terms

Shock-induced activation: Activation directly induced or modified by the shock.

Duration of shock-induced activation: Time interval between shock and 50% recovery of shock-induced activation.

First postshock activation: Activation that occurs after a shock-induced activation.

Postshock latency: Time interval between shock and onset of first postshock activation in the entire mapped region. This interval is equivalent to the "isoelectric window" determined by use of electrode mapping techniques (see reference 1).

Quiescent period: Time interval between repolarization of shock-induced activation and onset of first postshock activation. If the latter occurred earlier than the former (no quiescent window), a negative number was used for the quiescent period.

Type A defibrillation: Successful defibrillation without any first postshock activation (see reference 1).

Type B defibrillation: Successful defibrillation characterized by >1 rapid postshock activation before electrical quiescence (see reference 1).

Results

In all RVs, VF was repeatedly inducible throughout the experiment (3.8 ± 1.1 hours) by shocks during the vulnerable period. A total of 78 ± 30 shocks were given per experiment (50 ± 14 defibrillation attempts and 36 ± 15 VF induction attempts). ULV (3.5 ± 1.0 J, 288 ± 44 V) correlated with DFT50 (2.5 ± 0.6 J, $245\text{ V}\pm 34$ V). *r* values ($n=8$) were $r=0.7$ ($P=0.03$) and $r=0.75$ ($P=0.03$), respectively. ULV was significantly higher ($P<0.05$ for both joules and volts) than DFT50. Triphenyl tetrazolium chloride staining showed that, in all RVs, mapped myocardium was viable (stained brick red).

Patterns of Activation During Unsuccessful Ventricular Defibrillation

We analyzed 409 episodes of defibrillation shocks. Among them, 313 were unsuccessful at defibrillation. Adequate optical maps were obtained in 108. When the shock strength was >100 V lower than DFT50 ($n=37$), most ($n=20$) of the episodes showed no quiescent period. Figure 1 shows an example. Yellow arrows indicate direction of propagation of a large wavefront. The wavefront (red line) 8 ms after shock marks the border of shock-depolarized area.⁴ Most of the border of shock-depolarized area failed to propagate into the left side of the mapped region (colored blue at 27 ms), whereas the center of the border of shock-depolarized area continued to propagate (yellow arrow at 47 ms). This resulted in a figure 8 pattern (66 and 74 ms, yellow arrows) without actual reentry. Green arrows at 27 and 66 ms show wavebreaks not seen before the shock in those locations. VF continued and defibrillation failed (124 through 229 ms). Figure 1B shows actual optical signals recorded during this failed episode. These patterns of activation were almost exactly the same as that reported in Figure 2 of a previous study in which electrode mapping techniques were used.³

For near-threshold (within 50 V of DFT50) failed defibrillation ($n=36$), a synchronized, shock-induced activation occurred followed by organized repolarization. In some episodes, shocks induced locally propagated activations.¹⁶ These shock-induced activations fully repolarized 64 ± 18 ms after

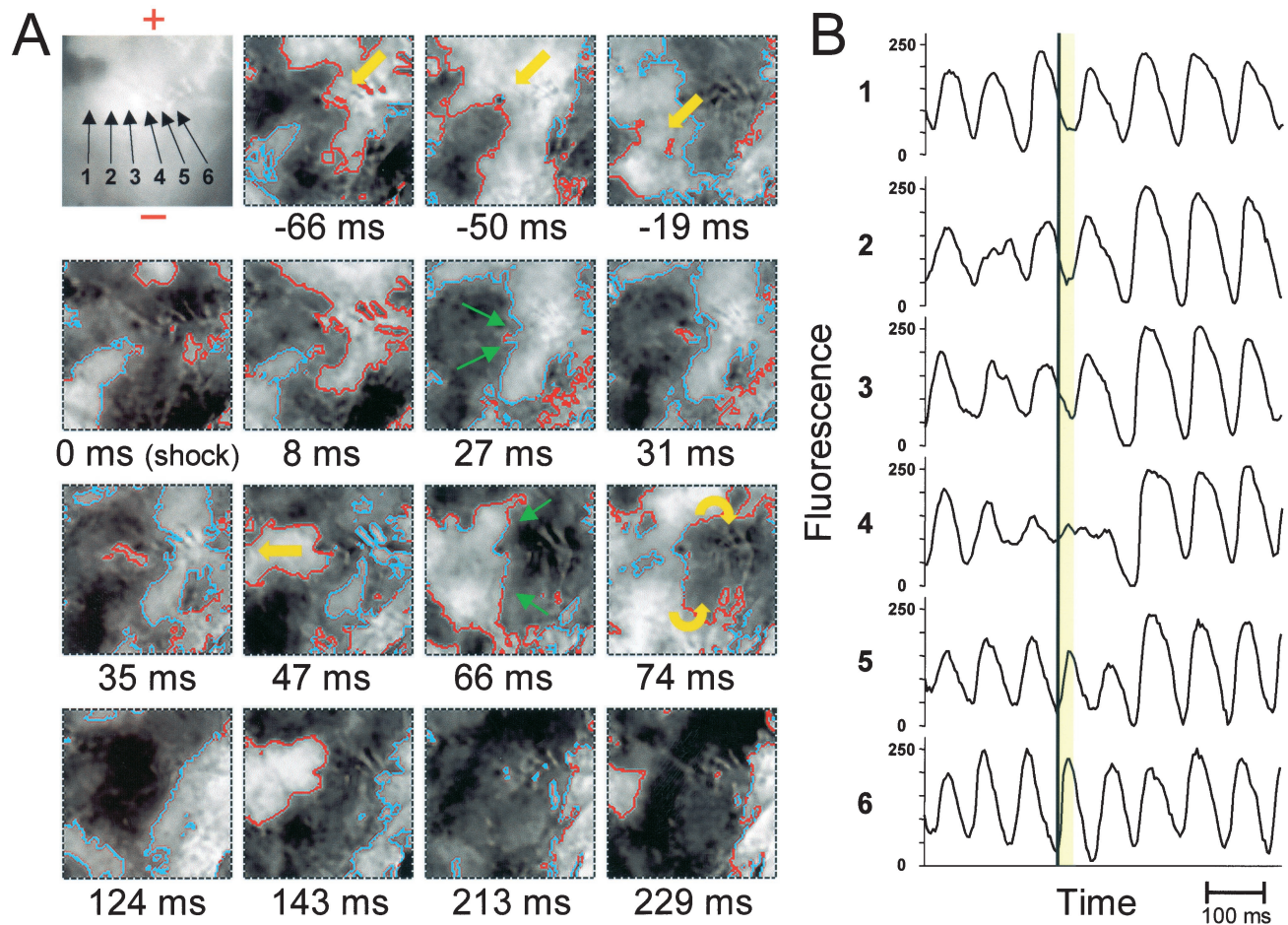


Figure 1. Unsuccessful defibrillation without quiescent period. Strength of shock was 150 V, or 190 V below DFT50 in that RV. A, First frame shows locations of the anode (+) and cathode (–) of defibrillation electrodes and 6 sites from which fluorescent signals in B were registered. Number below each frame shows time (time of shock is time zero). A, Creation of figure 8 reentry after shock. B, Actual optical signals registered, including that at core of reentry (site 4). Black line is time of shock; yellow highlight, postshock latency.

the shock. After a period of complete quiescence for 18 ± 24 ms, activation was reinitiated 83 ± 33 ms after shock. These postshock activations resulted in large and coherent wavefronts. Afterward, multiple-wavelet VF developed. Figure 2 shows an example. In Figure 2A, 2 wavefronts were moving toward the center before shock (yellow arrows). Wavebreaks (green arrows) were present. At the time of shock, a large portion of the mapped area was depolarized, as indicated by the gray scale. These patterns were followed by a period of quiescence, during which no wavefronts were present (frames for 43 through 58 ms). The first postshock activation occurred as an epicardial breakthrough 62 ms after the shock (white arrow) and propagated in the left upper direction (yellow arrows, frames for 78 and 81 ms). This 62-ms latency between shock and occurrence of first postshock activation is the optical equivalent of an isoelectric window.¹ Figure 2B shows actual optical recordings obtained during the same episode. Initial postshock organized activation soon degenerated back into multiple-wavelet VF. Wavebreaks were present in frames for 271 and 294 ms. These patterns of activation (isoelectric window followed by focal onset) were similar to those reported in Figure 4 of a previous study in which electrode-mapping techniques were used.³

Among unsuccessful defibrillation shocks, the first postshock activation in 57 episodes was nonfocal. In the remaining 51 episodes, the first postshock activation contained ≥ 1 focal pattern. No difference in the shock strengths existed between these groups (161 ± 72 versus 171 ± 59 V, respectively).

Duration of the postshock quiescent period and latency depended on strength of shocks. Figure 3 shows that as shock strength gradually increased, postshock latency lengthened. A weak positive correlation existed between shock strength and the quiescent period ($r=0.32$, $P<0.001$) and between shock strength and postshock latency ($r=0.56$, $P<0.0001$). The latter findings were compatible with results of electrode mapping studies.¹ When shock strength was <100 V (or >50 V $< \text{DFT50}$), the quiescent period was rarely observed.

Patterns of Activation During Successful Defibrillation

We recorded 74 episodes of type A and 22 episodes of type B successful defibrillation. Among them, 39 episodes of type A and 13 episodes of type B shocks had adequate optical recordings. Shock strength of type A defibrillation

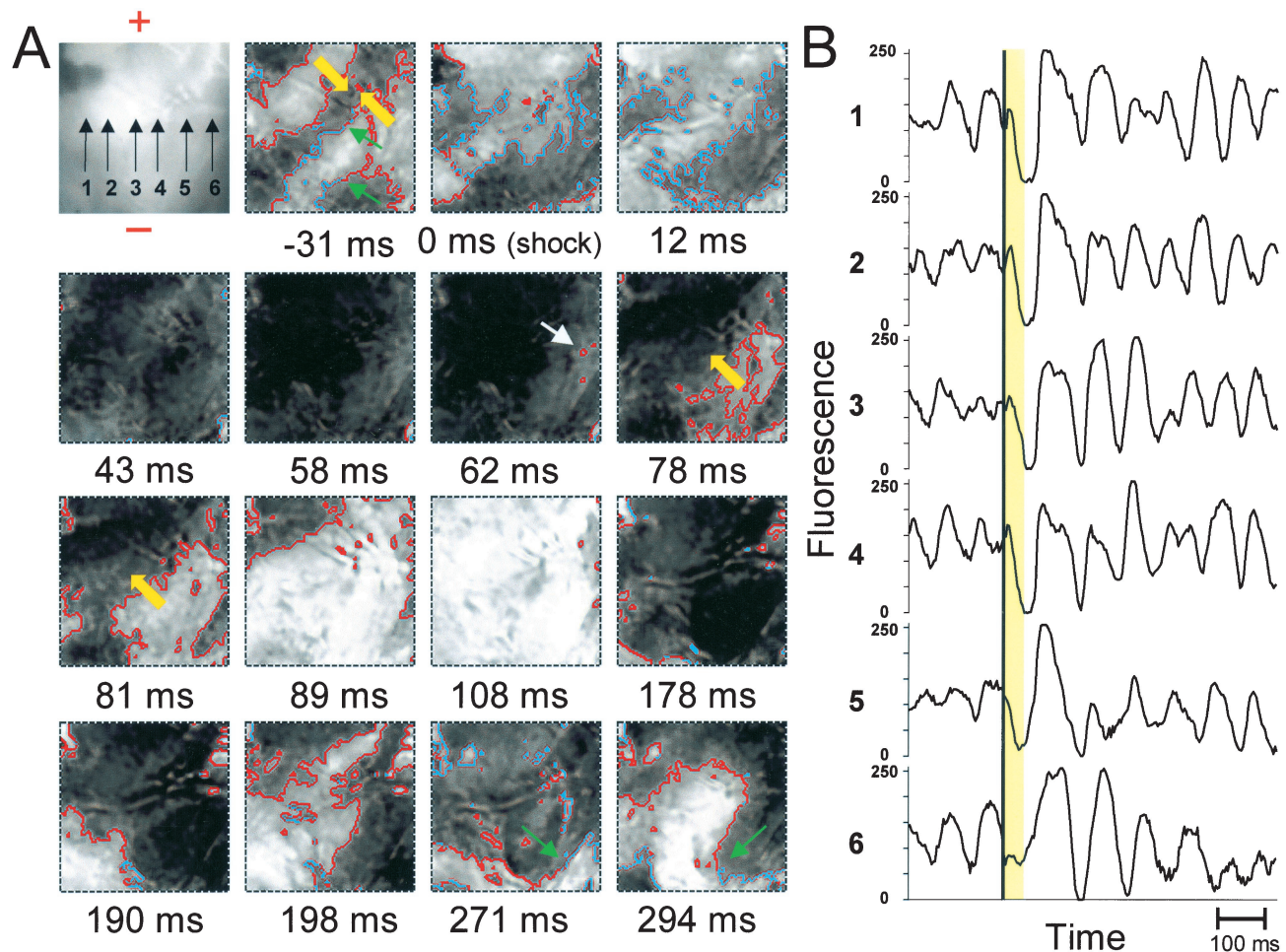


Figure 2. Quiescent period after near-threshold (200 V) unsuccessful shock. A, Patterns of activation before and after shock (time zero). A quiescent period (frames 43 through 58 ms) was followed by epicardial breakthrough (white arrow, frame 62 ms). B, Actual optical signals from locations in A, upper left. Black line is time of shock; yellow highlight, postshock latency.

(4.97 ± 2.23 J or 304.7 ± 76.8 V) was significantly higher than that of type B defibrillation (2.93 ± 1.43 J or 259.1 ± 54.9 V, $P < 0.05$) and unsuccessful defibrillation (2.15 ± 1.67 J or 196.6 ± 77.7 V, $P < 0.01$). Type B successful defibrillation always occurred when shock strength was within 70 V of DFT50. Type B episodes were associated with 2.8 ± 1.9 activations after shock before complete termination of all electrical activities. The first postshock activation always occurred after all wavebacks (blue lines) disappeared from the epicardium. Patterns of activation after type B successful defibrillation and those after unsuccessful near-threshold defibrillation were similar except for duration of shock-induced activation and activation cycle length (Table).

Induction of VF by Shocks During the Vulnerable Period of Paced Rhythm

Patterns of activation at induction of VF were similar to that observed after a near-threshold unsuccessful shock or immediately after Type B defibrillation. Figure 4 shows a typical example. In Figure 4A, before a 250-V shock in the relative refractory period, RV was activated by a single large wavefront originating from the pacing site on the lower edge of the

RV. A shock with a coupling interval of 240 ms resulted in immediate activation of a large amount of the ventricular tissue. Afterward, quiescence occurred over most of the mapped region (frames for 58 through 62 ms). The first postshock activation occurred as an epicardial breakthrough 66 ms after the shock (white arrow). In comparison, a 250-V shock during VF in the same RV also resulted in depolarization and repolarization (frames for 0 and 8 ms, Figure 4B) followed by a quiescent period (frames for 47 and 58 ms). Afterward, a large wavefront originating from the right edge of the mapped region (arrow, frame for 62 ms) reinitiated VF. A summary of all episodes of VF induction by near-threshold strength shocks can be found in the Table.

Discussion

Using optical mapping techniques, we found that near-threshold unsuccessful defibrillation shocks terminated all activation wavefronts of VF. After repolarization of shock-induced activations, a period of quiescence occurred during which no propagating wavefronts or wavebacks existed. VF was reinitiated after a postshock latency (an optical equivalent of the isoelectric window) by new wavefronts that

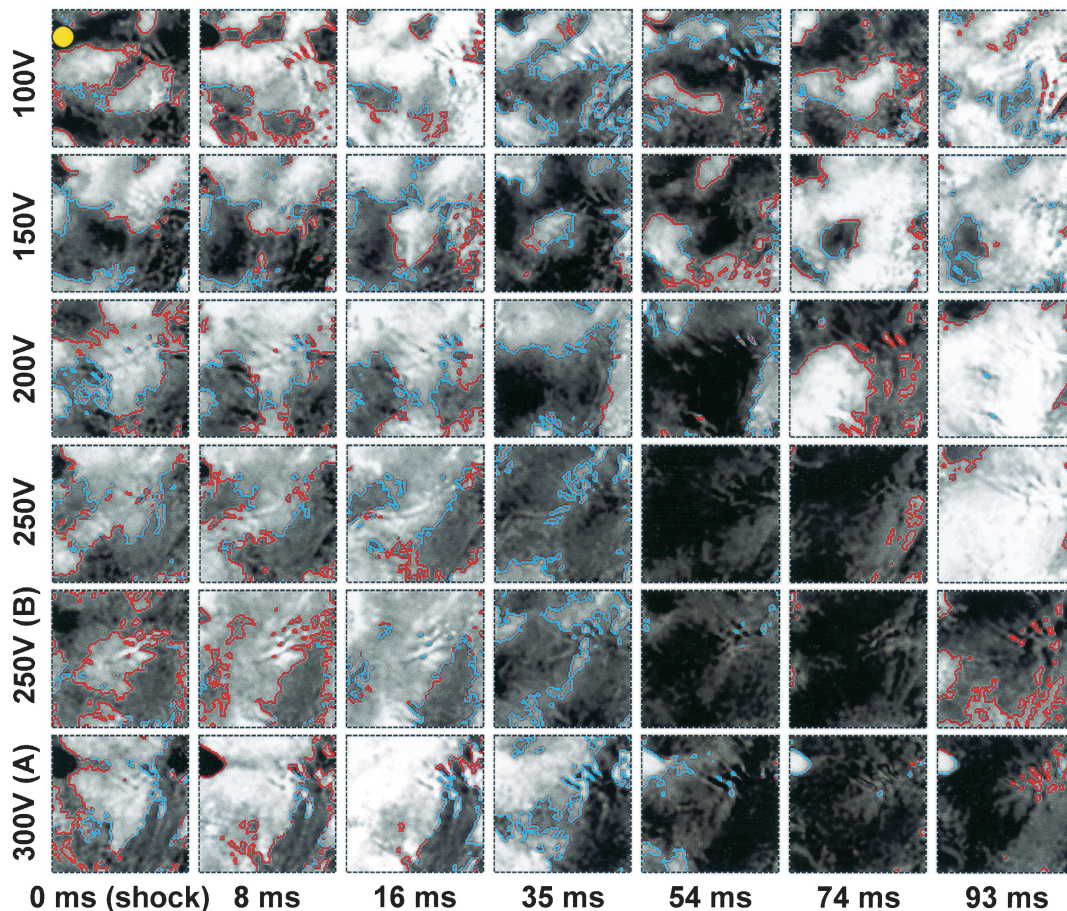


Figure 3. Effects of shock strength on quiescent period and postshock latency. DFT50 of this RV was 340 V. Figure shows a composite of optical maps associated with shocks of different strengths, as indicated on left. Shock occurred at time zero. Note that with low shock strength, no quiescent period occurred. As shock strength increased, a quiescent period became apparent and postshock latency increased. Large yellow dot in the first frame shows location of LED light. When light comes on during shock, a black dot is registered. Artifacts occurred on the right edge of the mapped region (red line segments at 93 ms, right lower subpanel). Artifacts were seen only after a successful shock. A indicates type A success; B, type B success.

propagated in directions different from those of the immediate preshock activations. Similar patterns of activation were observed after shocks that induced VF in the vulnerable period of paced rhythm. We conclude that an optical equivalent of an isoelectric window exists after near-threshold defibrillation shocks. These findings support the notion that a near-threshold unsuccessful defibrillation shock terminates all activation wavefronts but fails to halt VF because the same shock reinitiates VF after an isoelectric window.

Optical Equivalent of an Isoelectric Window

Results of the present studies were inconsistent with those reported by Kwaku and Dillon.^{4,5} However, Gray et al¹⁷ reported a long postshock quiescent period (110 ms) after unsuccessful atrial defibrillation shocks. One explanation for these discrepancies is that the mechanisms of atrial and ventricular defibrillation are completely different. Presence of a long postshock quiescence in atrial defibrillation does not necessarily mean that ventricular defibrillation is associated with the same pattern.

A second possible explanation is that Kwaku and Dillon⁴ did not recognize the difference between shock-induced

activation and the first postshock activation. Shock-induced activations propagate from the border of shock-depolarized area⁴ and form wavebreaks, critical points,¹⁸ or phase singularities.¹⁹ A wavebreak, critical point, or phase singularity induced by weak shocks could be associated with formation of reentrant excitation leading to induction of VF. Optical mapping could not demonstrate an isoelectric window when weak shocks were applied (Figure 1A). However, for near-threshold shocks, success or failure of defibrillation was not determined by shock-induced wavebreaks. As shown in Figure 2A, the wavefronts induced by the shock itself propagated and terminated without inducing VF. After cessation of these locally propagated activations, a quiescent period occurred followed by a new wavefront that reinitiated VF. Therefore, VF was reinitiated after all wavebreaks and wavefronts induced directly by the shock had terminated.

A third possible explanation is that Kwaku and Dillon⁴ did not analyze the differences in activation patterns according to the strength of shocks. In Figure 6 of that report, after a shock-induced depolarization, a period of electrical quiescence occurred until activation broke through, 57 ms after

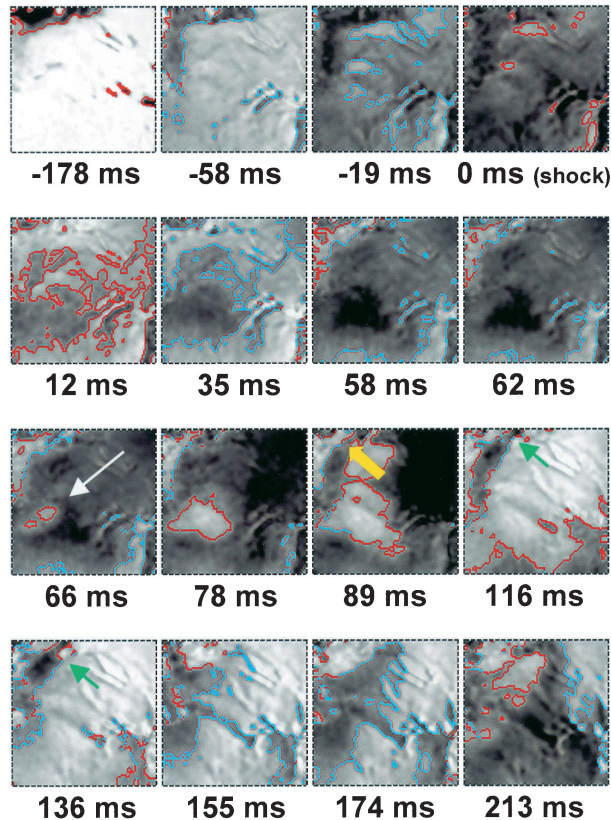
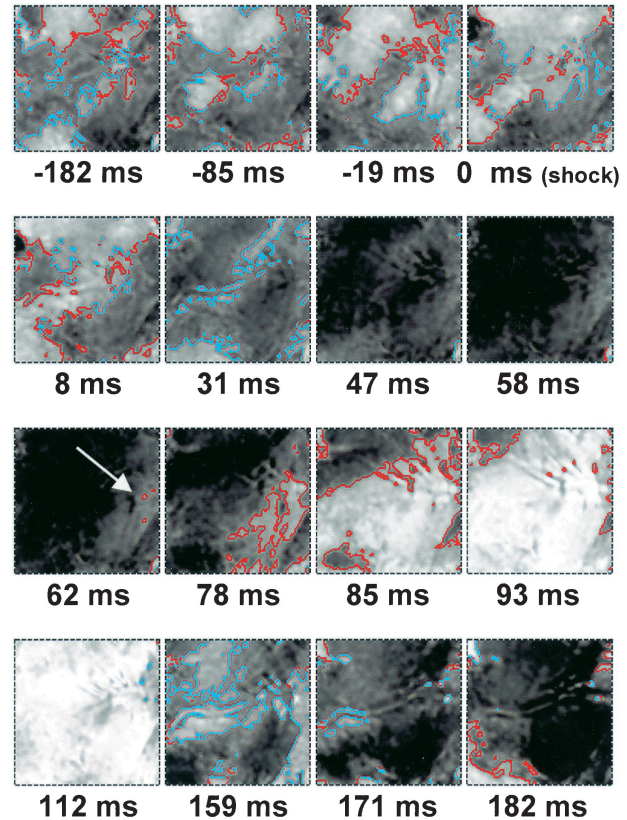
A. Induction of VF (250 V)**B. Unsuccessful Defibrillation (250 V)**

Figure 4. Comparison between induction of VF from sinus rhythm (A) and induction of VF from VF (unsuccessful defibrillation, B). Time of shock was time zero.

shock. We propose that this latter activation is equivalent to the first postshock activation after a strong shock^{1,3} and that an optical equivalent of an isoelectric window might be present in their studies.

Possible Mechanisms of Postshock Reinitiation of VF After Isoelectric Window

Gray et al¹⁷ suggested that ectopic beats induced by strong electrical shocks²⁰ could account for the first postshock activation. If this is true, increasing shock strength should be

associated with more ectopic activities. However, increasing shock strength is usually associated with complete elimination of postshock activities (type A defibrillation).¹

A second possible explanation for postshock activation is a shock-induced virtual electrode mechanism.¹⁹ Although virtual electrodes occur immediately after shock, their effects on membrane potential might last until after the end of shock. For example, wavefronts induced by virtual electrodes could move slowly at the boundary between hyperpolarized and depolarized regions before

Characteristics of Postshock Activities in Defibrillation and VF Induction With Near-Threshold Shocks

	Type B Successful Defibrillation (n=13)	Near-Threshold Unsuccessful Defibrillation (n=36)	Induction of VF by Near-Threshold Shocks (n=13)	P
Shock strength, V	259±55	246±62	242±49	NS
Duration of shock-induced activation, ms	78±24*	64±18*	123±44	<0.001
Quiescent period, ms	20±13	18±24†	-1±29	0.039
Postshock latency, ms	98±27	83±33*	122±55	0.007
Activation cycle length (first 3 after shock), ms	143±31	110±36‡	143±22	<0.001

* $P<0.01$, † $P<0.05$ vs induction shocks, ‡ $P<0.01$ vs other groups.

propagating away from this boundary at a more normal velocity. During the slow propagation from the boundary, an isoelectric window might be registered.

A third explanation of the isoelectric window is the propagated graded response hypothesis.^{21–23} Slowly propagating graded responses²³ keep local membrane potential elevated while the surrounding cells repolarize at a much faster rate. When graded responses finally encounter fully excitable tissue, they may reinitiate a regenerative response long after the time of the last electrical stimulation.^{21–23} Because graded responses are of low amplitude and propagate slowly, they might have been missed by both electrode and optical mapping techniques.

Limitations of the Study

To reduce motion artifacts, we and other investigators^{4,19} used DAM or calcium channel blockers to suppress tissue contraction. A benefit of using DAM in the present study is that we may compare our results with those of others. However, DAM and calcium channel blockers may alter patterns of activation during VF by flattening cardiac restitution.²⁴ A second limitation is that optical mapping techniques cannot detect wavefronts transmurally. During the isoelectric window, wavefronts possibly could have propagated outside of the mapped region and reactivated the mapped area by transmural propagation. Shocks also could have resulted in wavebreak and reentry in the midmyocardium, which cannot be mapped with the optical mapping techniques used in the present study. However, previous studies with sock-and-plunge electrodes^{1,3} showed no evidence of wavefront propagation or reentry during the isoelectric window.

Acknowledgments

The present study was supported by a fellowship grant from College of Medicine, Yonsei University, Seoul, Korea (Dr Lee); a Cedars-Sinai Electronic Heart Beat (ECHO) Foundation award, Los Angeles, Calif (Dr Karagueuzian); a Pauline and Harold Price endowment, Los Angeles, Calif (Dr Chen); NIH grants P50-HL-52319, HL-66389, HL-58533, and HL-58241; AHA grants 9750623N and 9950464N; University of California-Tobacco Related Diseases Research Program 9RT-0041; and the Ralph M. Parsons Foundation, Los Angeles, Calif. We thank Scott Lamp, Alan Garfinkel, PhD, and James N. Weiss, MD, for developing the software used for wavefront analyses. We also thank Ling-Tao Fan, Avile McCullen, and Meiling Yuan for their technical assistance and Elaine Lebowitz for her secretarial assistance.

References

- Chen P-S, Shibata N, Wolf P, et al. Activation during ventricular defibrillation in open-chest dogs: evidence of complete cessation and regeneration of ventricular fibrillation after unsuccessful shocks. *J Clin Invest*. 1986;77:810–823.
- Shibata N, Chen P-S, Dixon EG, et al. Epicardial activation following unsuccessful defibrillation shocks in dogs. *Am J Physiol*. 1988;255:H902–H909.
- Chen P-S, Wolf PD, Melnick SD, et al. Comparison of activation during ventricular fibrillation and following unsuccessful defibrillation shocks in open chest dogs. *Circ Res*. 1990;66:1544–1560.
- Kwaku KF, Dillon SM. Shock-induced depolarization of refractory myocardium prevents wave-front propagation in defibrillation. *Circ Res*. 1996;79:957–973.
- Dillon SM, Kwaku KF. Progressive depolarization: a unified hypothesis for defibrillation and fibrillation induction by shocks. *J Cardiovasc Electrophysiol*. 1998;9:529–552.
- Chen P-S, Swerdlow CD, Hwang C, et al. Current concepts of ventricular defibrillation. *J Cardiovasc Electrophysiol*. 1998;9:553–562.
- King BG. The effect of electric shock on heart action with special reference to varying susceptibility in different parts of the cardiac cycle [doctoral thesis]. New York, NY: Aberdeen Press, Columbia University; 1934.
- Fabiato PA, Coumel P, Gourgon R, et al. Le seuil de réponse synchrone des fibres myocardiques: application à la comparaison expérimentale de l'efficacité des différentes formes de chocs électriques de défibrillation. *Arch Mal Coeur*. 1967;60:527–544.
- Chen P-S, Shibata N, Dixon EG, et al. Comparison of the defibrillation threshold and the upper limit of ventricular vulnerability. *Circulation*. 1986;73:1022–1028.
- Chen P-S, Feld GK, Kriett JM, et al. Relation between upper limit of vulnerability and defibrillation threshold in humans. *Circulation*. 1993;88:186–192.
- Kim Y-H, Garfinkel A, Ikeda T, et al. Spatiotemporal complexity of ventricular fibrillation revealed by tissue mass reduction in isolated swine right ventricle: further evidence for the quasiperiodic route to chaos hypothesis. *J Clin Invest*. 1997;100:2486–2500.
- Lin S-F, Roth BJ, Wikswo JP Jr. Quatrefoil reentry in myocardium: an optical imaging study of the induction mechanism. *J Cardiovasc Electrophysiol*. 1999;10:574–586.
- Chen P-S, Feld GK, Mower MM, et al. Effects of pacing rate and timing of shock on the relationship between the defibrillation threshold and the upper limit of vulnerability in open chest dogs. *J Am Coll Cardiol*. 1991;18:1555–1563.
- Fishbein MC, Meerbaum S, Rit J, et al. Early phase acute myocardial infarct size quantification: validation of the triphenyl tetrazolium chloride tissue enzyme staining technique. *Am Heart J*. 1981;101:593–600.
- Voroshilovsky O, Qu Z, Lee M-H, et al. Mechanisms of ventricular fibrillation induction by 60-Hz alternating current in isolated swine right ventricle. *Circulation*. 2000;102:1569–1574.
- Chattipakorn N, KenKnight BH, Rogers JM, et al. Locally propagated activation immediately after internal defibrillation. *Circulation*. 1998;97:1401–1410.
- Gray RA, Ayers G, Jalife J. Video imaging of atrial defibrillation in the sheep heart. *Circulation*. 1997;95:1038–1047.
- Banville I, Gray RA, Ideker RE, et al. Shock-induced figure-of-eight reentry in the isolated rabbit heart. *Circ Res*. 1999;85:742–752.
- Efimov IR, Cheng YN, Biermann M, et al. Transmembrane voltage changes produced by real and virtual electrodes during monophasic defibrillation shock delivered by an implantable electrode. *J Cardiovasc Electrophysiol*. 1997;8:1031–1045.
- Jones JL, Lepeschkin E, Jones RE, et al. Response of cultured myocardial cells to countershock-type electric field stimulation. *Am J Physiol*. 1978;235:H214–H222.
- Van Dam RT, Moore NE, Hoffman BF. Initiation and conduction of impulses in partially depolarized cardiac fibers. *Am J Physiol*. 1963;204:1133–1144.
- Chen P-S, Cha YM, Peters BB, et al. Effects of myocardial fiber orientation on the electrical induction of ventricular fibrillation. *Am J Physiol*. 1993;264:H1760–H1773.
- Gotoh M, Uchida T, Mandel WJ, et al. Cellular graded responses and ventricular vulnerability to reentry by a premature stimulus in isolated canine ventricle. *Circulation*. 1997;95:2141–2154.
- Riccio ML, Koller ML, Gilmour RFJ. Electrical restitution and spatio-temporal organization during ventricular fibrillation. *Circ Res*. 1999;84:955–963.